mathematics

MDPI

Article

Temporal Community Detection and Analysis with Network Embeddings

Limengzi Yuan [1,†], Xuanming Zhang [1,†,‡], Yuxian Ke [1], Zhexuan Lu [1], Xiaoming Li [2,*] and Changzheng Liu [1,*]

[1] College of Information Science and Technology, Shihezi University, Xinjiang 832003, China; ylmz@shzu.edu.cn (L.Y.); zhangxm236@mail2.sysu.edu.cn (X.Z.); keyuxian520805@outlook.com (Y.K.); 20221010063@stu.shzu.edu.cn (Z.L.)
[2] College of International Business, Zhejiang Yuexiu University, Shaoxing 312000, China
* Correspondence: lxm696@tju.edu.cn (X.L.); liucz@shzu.edu.cn (C.L.)
† These authors contributed equally to this work.
‡ Current address: School of Artificial Intelligence, Sun Yat-sen University, Zhuhai 510275, China.

Abstract: As dynamic systems, social networks exhibit continuous topological changes over time, and are typically modeled as temporal networks. In order to understand their dynamic characteristics, it is essential to investigate temporal community detection (TCD), which poses significant challenges compared to static network analysis. These challenges arise from the need to simultaneously detect community structures and track their evolutionary behaviors. To address these issues, we propose TCDA-NE, a novel TCD algorithm that combines evolutionary clustering with convex non-negative matrix factorization (Convex-NMF). Our method innovatively integrates community structure into network embedding, preserving both microscopic details and community-level information in node representations while effectively capturing the evolutionary dynamics of networks. A distinctive feature of TCDA-NE is its utilization of a common-neighbor similarity matrix, which significantly enhances the algorithm's ability to identify meaningful community structures in temporal networks. By establishing coherent relationships between node representations and community structures, we optimize both the Convex-NMF-based representation learning model and the evolutionary clustering-based TCD model within a unified framework. We derive the updating rules and provide rigorous theoretical proofs for the algorithm's validity and convergence. Extensive experiments on synthetic and real-world social networks, including email and phone call networks, demonstrate the superior performance of our model in community detection and tracking temporal network evolution. Notably, TCDA-NE achieves a maximum improvement of up to 0.1 in the normalized mutual information (NMI) index compared to state-of-the-art methods, highlighting its effectiveness in temporal community detection.

Keywords: temporal community detection; social networks; network embedding; evolutionary clustering; convex non-negative matrix factorization

MSC: 90C35

check for updates

Academic Editor: Andrea Scozzari

Received: 2 January 2025
Revised: 15 February 2025
Accepted: 17 February 2025
Published: 21 February 2025

Citation: Yuan, L.; Zhang, X.; Ke, Y.; Lu, Z.; Li, X.; Liu, C. Temporal Community Detection and Analysis with Network Embeddings. *Mathematics* **2025**, *13*, 698. https://doi.org/10.3390/math13050698

Copyright: © 2025 by the authors. Licensee MDPI, Basel, Switzerland. This article is an open access article distributed under the terms and conditions of the Creative Commons Attribution (CC BY) license (https://creativecommons.org/licenses/by/4.0/).

1. Introduction

With the rapid advancement of internet and 5G communication technologies, social networks have grown increasingly complex and dynamic. These networks encompass diverse forms, including author collaboration networks (comprising authors and articles), social communication platforms (e.g., WeChat, QQ, Facebook, WhatsApp), blogging platforms (e.g., Weibo, X), self-media channels (e.g., Bilibili, YouTube), and professional

mobility networks (e.g., LinkedIn). These platforms serve as critical links both within and between groups, embedding rich information about community structures and complex relationships. The extraction and analysis of such information holds significant academic and practical value, enabling efficient mining of actionable data and uncovering patterns in community evolution. This in turn supports more accurate predictions of future trends [1].

While previous research on community detection has predominantly focused on static networks [2], there is increasing acknowledgment of the dynamic nature of network structures. Most real-world networks, such as transportation and social networks, are inherently dynamic, being characterized by evolving node attributes, relationships, and community structures [3,4]. This dynamism introduces unique challenges in community detection, particularly in capturing the temporal evolution of networks. Specifically, the dynamic nature of network structures, manifested through variations in the number of nodes and communities as well as changes in link densities between nodes, gives rise to evolutionary behaviors [4]; furthermore, community sizes expand as data volumes grow, leading to increased time and space complexity in traditional methods [5,6], which ultimately results in inefficient community detection.

A key innovation of our method lies in the integration of network embedding (NE), which maps network nodes to continuous low-dimensional representations, thereby enhancing the capture of structural features within the network [7–10]. TCDA-NE employs an advanced NE technique that integrates both first-order and second-order proximities [11,12], effectively transforming the high-dimensional sparse vector space of the network into a low-dimensional dense representation. This transformation facilitates more comprehensive and precise extraction of the fundamental structural characteristics of the original network, particularly in the context of temporal evolution. To address the challenges of community detection in complex networks, we utilize non-negative matrix factorization (NMF) [4,13,14], which not only improves computational efficiency and simplifies matrix operations but also enhances the interpretability of the decomposition results. Specifically, TCDA-NE incorporates Convex-NMF, which imposes convex constraints on the centroid matrix to effectively mitigate the persistent issue of data sparsity in dynamic networks [15,16]. Our study investigates various combinations of NMF methods and network embedding techniques, with a particular emphasis on integrating first-order and second-order proximities in temporal community detection using Convex-NMF. The results demonstrate the efficacy of this approach in preserving microscopic topological structures, accurately capturing node relationships, and addressing data sparsity challenges in dynamic network analysis. The key contributions of this study are as follows:

1. **Enhanced Network Representation:** We propose a novel approach integrating network embedding (NE) with first-order and second-order proximity considerations. We generate more effective node embeddings by employing a similarity matrix rather than a traditional adjacency matrix, facilitating more precise representation of the network's microscopic community structure. This approach significantly enhances the quality of community detection in complex networks.
2. **Advanced Temporal Community Detection:** Unlike traditional two-step or incremental clustering methods, TCDA-NE utilizes evolutionary clustering to enforce temporal smoothness between consecutive time steps. This innovative strategy enables more refined and precise tracking of community evolution in dynamic networks, effectively addressing a critical challenge in temporal network analysis.
3. **Optimized Matrix Factorization:** We employ Convex-NMF to derive community membership matrices, which exhibit superior performance over Semi-NMF and other mainstream NMF methods. This optimization substantially improves both the

quality and interpretability of community detection results, especially in the context of temporal networks.

4. **Comprehensive Experimental Validation:** The effectiveness of TCDA-NE is rigorously validated through comprehensive experiments on both real-world and synthetic datasets. We propose a novel evaluation framework that assesses static and dynamic performance metrics. The results conclusively show that TCDA-NE not only surpasses existing methods in community detection quality but also demonstrates superior dynamic performance, which is primarily attributed to its integration of temporal smoothness constraints.
5. **Bridging Static and Dynamic Network Analysis:** TCDA-NE represents a significant advancement in bridging the gap between static and dynamic network analysis techniques. By integrating advanced network embedding, evolutionary clustering, and optimized matrix factorization, our method provides a more holistic approach to understanding complex network dynamics over time.

The remainder of this paper is structured as follows: Section 2 presents an overview of related work on temporal community detection and network embedding; Section 3 outlines the objective function and provides a theoretical analysis of the proposed algorithm; Section 4 describes experiments conducted on multiple datasets; finally, Section 5 presents our conclusions.

2. Related Work

The related work involves the two primary areas: temporal community detection and network embedding methods for temporal networks.

2.1. Temporal Community Detection

Temporal community detection is a model specifically tailored to analyze community structures in temporal networks, where a community organization undergoes temporal variations with each time step. Methods developed in recent years fall into two categories.

2.1.1. Methods Based on Heuristic Optimization

In the context of temporal community detection, heuristic optimization approaches can be classified into three main categories: two-stage methods, incremental clustering-based methods, and evolutionary clustering techniques.

Two-stage or two-step methods. These approaches address community detection and its evolution as distinct tasks. Specifically, community detection is conducted independently at each time step and similarity measures are utilized to establish correspondences between communities across different time steps. Yang et al. [17] proposed an innovative approach by integrating multiple strategies into a community-related link prediction method enhanced with an evolutionary process in order to effectively improve the identification of ambiguous community structures in complex networks. Extending this work, Cha et al. [18] implemented two-step methods for early-stage depression detection. Furthermore, Odhiambo et al. [19] evaluated a two-step case-finding approach designed to address the healthcare needs and challenges faced by this population, particularly in the context of obstructive respiratory diseases.

Incremental clustering-based methods. These methods are typically initiated with a community structure derived from a static network at the first time step, and subsequently adapt community assignments as the network evolves. DynaMo [20], an incremental clustering method based on modularity, demonstrates superior computational efficiency compared to the Louvain algorithm [21], particularly in identifying emerging activity classes while preserving established ones. McGann et al. [22] and Guo et al. [23] also

proposed models that utilize incremental clustering. In 2023, Li et al. [24] introduced an incremental clustering algorithm based on big data representative points and covariance (IDPC-RC). This method selects representative points from the initial dataset, calculates the similarity between new data points and these points to identify preassigned clusters, and adaptively adjusts the number of clusters using a covariance row-column formula. However, the reliance on covariance makes the algorithm highly sensitive to noise, and it may underperform in noisy environments, where even minor data perturbations can lead to inaccurate clustering results.

Evolutionary Clustering. Clustering at any given time step should accurately reflect current data while minimizing abrupt changes, thereby achieving lower historical costs and higher snapshot quality through the incorporation of regularization terms. Classical methods include FacetNet and DYNMOGA [25]. Furthermore, a series of multi-objective evolutionary clustering algorithms have been proposed, such as DECS [26] and DYNMODPSO [27]. Martinet et al. [28] developed a methodology to address the challenges associated with noisy networks, while Sapci [29] identified gene modules exhibiting temporal and inter-subject variability.

In summary, some previous methods overlook the temporal evolution of community information in dynamic networks, while others treat community detection and evolution as separate issues. Furthermore, certain approaches lack a comprehensive theoretical framework to address the joint problem of community detection and evolution.

2.1.2. Generative Models

Model generation is meant to establish the mechanism for generating dynamic complex networks, simulate the network formation process, and transform community detection into a parameter estimation problem. There are two categories of generation models.

Latent space approaches [30]. Sewell et al. [31] utilized an embedding approach to transform a dynamic network into a Euclidean space, enabling the detection of communities within dynamic friendship networks and global export–import data. Passino and Heard [32] proposed a Bayesian model to estimate the latent dimensions and communities in stochastic block models. Akcay et al. [33] used a semi-supervised learning framework for anomaly detection, leveraging generative adversarial networks (GANs) to effectively detect anomalies in various domains. Similar approaches were proposed in 2021, such as PAE and DLSM [34]. Recently, Xu et al. introduced bi-layer dynamic network embedding (Bi-DNE) [35] for preserving evolutionary patterns in dynamic networks in 2024. This method captures both micro- and macro-level dynamics through reinforced triadic closure and dynamic power-law evolution, significantly improving performance in link prediction and temporal analysis.

Approaches based on Dynamic Stochastic Block Models. Schaub et al. [36] introduced an innovative method for recovering stochastic block models (SBMs) without the need for prior knowledge of the network structure. In recent years, several similar approaches have been developed, such as DSBM [6], BPPM [37], and MMSBM [38]. These methods are particularly noteworthy, as they incorporate various previous models as special cases.

2.2. Network Embedding

Network embedding methods aim to capture the low-dimensional representations of communities within a network. Community detection techniques that leverage network embedding models have significant applications in two primary domains.

2.2.1. Matrix Decomposition

These methods utilize the similarity matrix of a projection network to derive node embeddings and microscopic community structures. GraRep [39] is a learning algorithm that generates low-dimensional vertex representations for weighted graphs, aiming to create compact vectors that effectively represent the vertices in the graph while incorporating global structural information. The high-order proximity-preserved embedding (HOPE) method seeks to preserve asymmetric transitivity and capture high-order proximities in large-scale graphs. The SENE network embedding model [40] utilizes seed expansion sampling to effectively capture the structural information of communities in the network. Zhen D et al. [41] proposed a hierarchical community structure maintenance method for network embedding (HCNE), aiming to effectively preserve the intralayer and hierarchical community structures under multigranularity. Hierarchical network embedding methods such as HB-DSBM [42] and LONE-NMF [43] have subsequently been proposed.

2.2.2. Deep Neural Networks

Deep neural network technology has been integrated with network embedding to learn network representations. Classical machine learning methods such as representational learning, RF, and CNN [44] have also been incorporated into deep embedded networks. Wu et al. [45] explored a deep learning approach to recognize clinical entities, employing minimal feature engineering. Wang and Gao et al. focused on deep structured network embedding and deep attribute network embedding. Shen et al. [46] examined the classification of cross-network nodes, utilizing labeled information from a source network to classify unlabeled nodes in a target network. Kan et al. [47] introduced a novel approach for deep feature embedding in 2022. Recently, Kojaku et al. [48] proposed a method for network community detection via neural embeddings, demonstrating that shallow linear graph neural networks such as node2vec can achieve the information-theoretic limit of community detectability.

3. TCDA-NE Model

TCDA-NE is a dynamic community detection model that incorporates the community structure in network embedding to effectively preserve the microstructure and mesoscopic community structure. We leverage the node degree and the number of shared neighbors to quantify the node similarity. In addition, we gradually optimize the community structure to address the challenge of network sparsity. Below, we explain the TCDA-NE model, including its formulation, derivation, solution, and pseudocode.

3.1. Model Description

Consider a dynamic undirected network $G = (V, E)$, where V and E represent the sets of nodes and edges, respectively. The network evolves over time, and this temporal aspect is captured by the binary adjacency matrix X_t, where t is time. At time t, the matrix element $X_{t,ij}$ in the complex network matrix indicates the presence or absence of a direct connection between nodes i and j, reflecting the existence or absence of an edge connecting them. If there is an edge, then $X_{t,ij} = 1$; otherwise, $X_{t,ij} = 0$. Similarly to the traditional model based on the non-negative convex matrix decomposition, the theoretical representation of TCDA-NE is shown in Figure 1.

Modeling community structure. By applying the principle of NMF, it becomes feasible to discover non-negative matrices W_t and G_t that provide an approximation of the matrix X_t through the relationship $X_t \approx X_t W_t G_t$. This factorization represents the decomposition of a non-negative matrix into the product of two non-negative matrices. The non-negativity property of W_t and G_t implies that W_t can be interpreted as a weight matrix, where the

numerical values of its nodes represent the weights assigned to them at time t; G_t captures the community membership, where $G_{t,ij}$ indicates the probability that node i belongs to the community j at time t. In particular, W_tG_t represents the centroid of the community. The centroid matrix F_t is defined as $F_t = X_tW_t$, where each column corresponds to the central node of a specific community. Thus, we can derive the function

$$\min_{X_t \geq 0} ||X_t - X_tW_tG_t^T||_F^2. \tag{1}$$

A temporal smoothness constraint is incorporated into the community membership matrix to consider the interdependence between consecutive time steps, quantifying the likelihood of significant changes in the community structure between times $t-1$ and t. The cost function encompasses modeling the network topology and the temporal smoothness constraint, combining the community discovery quality and historical cost. We aim to maximize community discovery quality while minimizing the historical cost; hence, we derive the cost function

$$\min_{W_t \geq 0, G_t \geq 0} ||X_t - X_tW_tG_t^T||_F^2 + \alpha||X_{t-1} - X_{t-1}W_{t-1}G_t^T||_F^2. \tag{2}$$

To quantify the importance of the temporal smoothness constraint, we introduce a temporal smoothness weight parameter, denoted as α. Typically, α assumes a value between 0 and 1. A more significant value of α indicates a higher weight for the temporal smoothness constraint in the cost function, meaning that the algorithm prioritizes the continuity and stability of the community structure across consecutive time steps. Consequently, during community detection, the algorithm minimizes significant changes in community structure between adjacent time steps, resulting in a smoother evolution of the community structure. Therefore, a higher value of α emphasizes the temporal smoothness constraint.

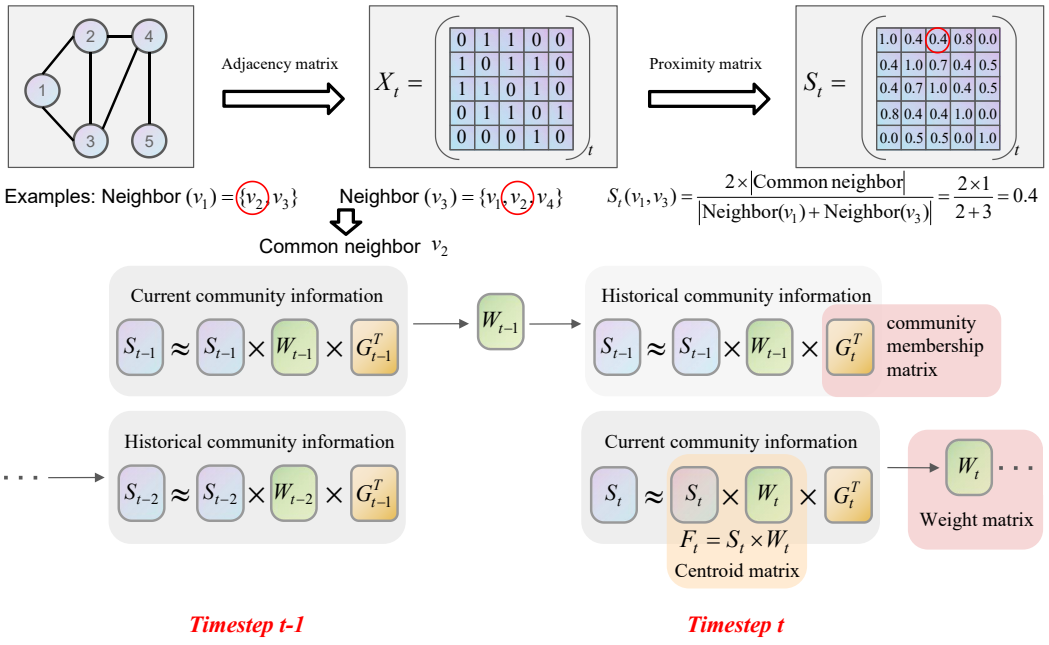


Figure 1. Model theory diagram of TCDA-NE.

Modeling microscopic structure. The first-order proximity $S^{(1)} = [S_{ij}^{(1)}]$ captures the most directly observed probability of proximity between two nodes. The value of X_{ij} indicates the existence or absence of first-order proximity between nodes i and j. When X_{ij} is greater than 0, this signifies the presence of first-order positive proximity, while a value of 0 indicates its absence.

We consider the adjacency matrix X to represent the first-order proximity. Preserving this is crucial, as it provides a direct representation of the proximity between nodes in a complex network. It has been demonstrated that the presence of a direct edge between two nodes implies their adjacency within a reduced-dimension vector space. However, in realistic scenarios complex networks often exhibit sparsity in observed edges, with only a limited number of edges connecting nodes; consequently, the absence of an edge does not necessarily indicate a lack of similarity. Hence, it is overly simplistic to rely solely on first-order proximity in low-dimensional settings to determine node similarity. A feasible solution is to utilize their common neighbor nodes. Specifically, two nodes with common neighbors are similar even if they have no directly connected edges, which yields the second-order proximity measure $S^{(2)} = [S_{ij}^{(2)}]$.

We represent the first-order proximity between node i and all other nodes as $N_i = (S_{i1}^{(1)}, S_{i2}^{(1)}, \ldots, S_{in}^{(1)})$. The second-order proximity is then determined by evaluating the similarity between N_i and N_j using the cosine similarity; here, for nodes i and j, $S_{ij}^{(2)} = \dfrac{N_i N_j}{||N_i||||N_j||}$, where $||N||$ is the norm of N. The utilization of cosine similarity ensures that the second-order proximity value falls within the range of 0 to 1.

To maintain the characteristics of both first- and second-order proximity, we introduce a weight parameter η to establish their relationship. Specifically, we define the combined proximity matrix as $S = S^{(1)} + \eta S^{(2)}$, where η is a positive constant that can be changed according to the situation. In our experiments, we set $\eta = 5$ in order to obtain better results.

To preserve both the community structure and the microscopic node properties of the network, we modify the original objective function by replacing W_t with the combined proximity matrix S_t, which integrates both the first- and second-order proximity. Thus, the following final objective function is obtained:

$$\min_{W_t \geq 0, G_t \geq 0} ||S_t - S_t W_t G_t^T||_F^2 + \alpha ||S_{t-1} - S_{t-1} W_{t-1} G_t^T||_F^2. \tag{3}$$

3.2. Model Solution

Next, we present the update rules for the variables W_t and G_t with respect to the objective function in (3) and prove their correctness by mathematical derivation. Due to the non-negative property of matrix factorization, there is no global optimal solution; however, when only one of the parameters is fixed, there is a local optimal solution.

When G_t is fixed and W_t is updated, we can write Equation (3) as follows:

$$\min_{W_t \geq 0, G_t \geq 0} ||S_t - S_t W_t G_t^T||_F^2. \tag{4}$$

To achieve the optimal solution, we incorporate the Lagrange multiplier matrix λ under a non-negativity constraint to ensure that S_t remains non-negative. By setting the Lagrange multiplier to zero, we can derive the following objective function:

$$H(W_t) = tr(-S_t^T S_t W_t G_t^T - G_t W_t^T S_t^T S_t + G_t W_t^T S_t^T S_t W_t G_t^T). \tag{5}$$

We assume $\dfrac{\partial H(W_t)}{\partial W_t} = 0$,

$$-2S_t^T S_t G_t + 2S_t^T S_t W_t G_t^T G_t = 0. \tag{6}$$

Introducing the KKT fixed point condition, we can obtain

$$-2S_t^T S_t G_t + 2S_t^T S_t W_t G_t^T G_t = \lambda_{ij} W_{t,ij} = 0, \tag{7}$$

which is equivalent to

$$(-2S_t^T S_t G_t + 2S_t^T S_t W_t G_t^T G_t)(W_{t,ij})^2 = 0. \tag{8}$$

Hence, the update transformation formula of W_t is

$$W_{t,ij} \leftarrow W_{t,ij}\left(\frac{(S_t^T S_t G_t)_{ij}}{(S_t^T S_t W_t G_t^T G_t)_{ij}}\right). \tag{9}$$

Similarly, when W_t is held constant and G_t is updated, we introduce a non-negative Lagrange multiplier matrix λ to enforce the non-negativity constraint on G_t, and obtain

$$\begin{aligned} H(G_t) = tr(&-S_t^T S_t W_t G_t^T - G_t W_t^T S_t^T S_t + G_t W_t^T S_t^T S_t W_t G_t^T \\ &- \alpha S_{t-1}^T S_{t-1} W_{t-1} G_t^T - \alpha G_t W_{t-1} S_{t-1}^T S_{t-1} \\ &+ \alpha G_t W_{t-1} S_{t-1}^T S_{t-1} W_{t-1} G_t^T). \end{aligned} \tag{10}$$

We assume $\dfrac{\partial H(G_t)}{\partial G_t} = 0$,

$$\begin{aligned} &- 2S_t^T S_t W_t + 2G_t W_t^T S_t^T S_t W_t - 2\alpha S_{t-1}^T S_{t-1} W_{t-1} \\ &+ 2\alpha G_t W_{t-1} S_{t-1}^T S_{t-1} W_{t-1} = 0. \end{aligned} \tag{11}$$

Introducing the KKT fixed point condition, we can obtain

$$\begin{aligned} &- 2S_t^T S_t W_t + 2G_t W_t^T S_t^T S_t W_t - 2\alpha S_{t-1}^T S_{t-1} W_{t-1} \\ &+ 2\alpha G_t W_{t-1} S_{t-1}^T S_{t-1} W_{t-1} = \lambda_{ij} G_{t,ij} = 0, \end{aligned} \tag{12}$$

which is equivalent to

$$\begin{aligned} (&- 2S_t^T S_t W_t + 2G_t W_t^T S_t^T S_t W_t - 2\alpha S_{t-1}^T S_{t-1} W_{t-1} \\ &+ 2\alpha G_t W_{t-1} S_{t-1}^T S_{t-1} W_{t-1})(G_{t,ij})^2 = 0. \end{aligned} \tag{13}$$

Hence, the update transformation formula fo G_t can be expressed as

$$G_{t,ij} \leftarrow G_{t,ij}\left(\frac{(S_t^T S_t W_t + \alpha S_{t-1}^T S_{t-1} W_{t-1})_{ij}}{(G_t W_t^T S_t^T S_t W_t + \alpha G_t W_{t-1}^T S_{t-1}^T S_{t-1} W_{t-1})_{ij}}\right). \tag{14}$$

Based on the above update rules, an iterative algorithm can be derived to optimize the TCDA-NE model, which is presented as Algorithm 1.

3.3. Temporal Complexity

Here, we analyze the temporal complexity associated with the update formulation. In Equation (9), $S_t^T(S_t G_t)$ and $S_t^T(S_t W_t)(G_t^T G_t)$ have temporal complexities of $O(4v_1k)$ and $O(4v_1k + 2ek_2)$, respectively. Similarly, in Equation (14), $S_{t-1}^T(S_{t-1}W_{t-1})$, $S_t^T(S_t W_t)$, $G_t((W_{t-1}^T S_{t-1}^T), (S_{t-1}W_{t-1}))$, and $G_t((W_t^T S_t^T)(S_t W_t))$ have respective complexities of $O(4v_1k)$, $O(4v_2k)$, $O(4v_1k + 2ek^2)$, and $O(4v_2k + 2ek^2)$. Here, v_1 and v_2 refer to the edge counts of the network at times t and $t-1$, respectively. The variable e is the number of nodes within the network, while k is the count of communities under consideration.

As a result, the temporal complexities of Equations (9) and (14) are $O(v_1k + ek_2)$ and $O(v_1k + v_2k + ek_2)$, respectively. The overall temporal complexity of TCDA-NE is $O(N(v_1k + v_2k + ek_2))$, where N is the total number of iterations required for convergence. Consequently, with a larger number of communities, the temporal complexity of TCDA-NE

exhibits significant variation. In theory, it has more advantages when the network is much larger than the community.

Algorithm 1: TCDA-NE model

Input: X_t, X_{t-1}, α, η
Complex network adjacency matrix at time step t, X_t;
Complex network adjacency matrix at time step t-1, X_{t-1};
Weight parameter of temporal smoothness α;
Tradeoff parameters for first- and second-order proximities η.
Output: G_t, W_t
Community membership matrix G_t corresponding to time t.
Weight matrix W_t corresponding to time t.

Compute multi-order proximity matrices S_{t-1}, S_t based on adjacency matrices X_{t-1}, X_t.
while *the objective function does not converge* **do**
  $W_{t,ij} \leftarrow W_{t,ij}\left(\frac{(S_t^T S_t G_t)_{ij}}{(S_t^T S_t W_t G_t^T G_t)_{ij}}\right)$
  $G_{t,ij} \leftarrow G_{t,ij}\left(\frac{(S_t^T S_t W_t + \alpha S_{t-1}^T S_{t-1} W_{t-1})_{ij}}{(G_t W_t^T S_t^T S_t W_t + \alpha G_t W_{t-1}^T S_{t-1}^T S_{t-1} W_{t-1})_{ij}}\right)$
  Normalize such that $\sum_j W_{ij} = 1, \forall i$.
return W_t, G_t

4. Experiments

Based on five network datasets (three real and two synthetic), we conducted experiments to compare current benchmark methods and widely accepted traditional methods and evaluate the performance of TCDA-NE in dynamic network community detection and function convergence.

4.1. Baselines and Settings

Dynamic community detection methods are based on concepts such as evolutionary clustering, genetic algorithm-based techniques, fusion clustering, modularity computation, genome representation, and convex non-negative matrix factorization; their outcomes serve as benchmarks for the identification of communities in dynamic complex networks. The comparison models in our experiments were as follows:

- **Facenet** [25] utilizes evolutionary clustering to analyze the dynamics of virtual communities, examining their evolution within a unified framework. It uses MAP estimation, incorporating both observed network data and a priori distributions derived from the historical community structure.
- **DYNMOGA** [25] uses a genetic algorithm-based approach to address the task of community discovery in dynamic networks. It formulates community detection with temporal smoothing as a multi-objective problem.
- **AFFECT** [49] uses shrinkage estimation to dynamically estimate the optimal smoothing parameters. This framework allows for the comparison of static clustering algorithms. In this paper, we use K-means clustering and spectral clustering extended to evolutionary clustering algorithms, denoted as AFFECT_kmeans and AFFECT_spectral, respectively.
- **DECS** [26] is a genome-based multi-objective evolutionary clustering algorithm that takes modular computation based on genomic matrices as an optimization objective.

- **ECD** [50] adopts a decomposition framework with a genomic representation to address the task of evolutionary community detection. It formulates the problem as a multi-objective optimization one, aiming to identify the evolutionary patterns of communities in dynamic social networks.
- **CDNMF** [51] is a novel algorithm for community detection that enhances the feature representation capability of non-negative matrix factorization (NMF) by integrating deep learning and contrastive learning mechanisms to more accurately identify community structures in networks.
- **FBCD** [52] is a community detection algorithm that integrates graph embedding models with node proximity measures to leverage both node attributes and network structure for enhanced accuracy in detecting communities within social networks.
- **StaNMF** [53] is a two-step approach for community detection based on stochastic non-negative matrix factorization (StaNMF), which initially divides the snapshot and subsequently applies NMF to detect communities in each time step.
- **DCNMF** [54] improves upon traditional community detection algorithms based on NMF by employing evolutionary clustering and convex non-negative matrix decomposition, leading to enhanced accuracy.
- **Semi-NMF** [54] is an evolutionary clustering-based algorithm for community detection that operates at both the community and node levels.

To obtain fair results, we used the authors' published source code and the published default parameters. Based on the convex non-negative matrix factorization method combining NE, we applied random initialization to the solution of NMF in each time step of all datasets. To mitigate the risk of TCDA-NE converging to a local minimum, we conducted 20 experimental runs and computed the average results, thereby enhancing the accuracy of the outcomes.

4.2. Performance Metrics and Datasets

We introduce three metrics that are widely employed to assess the efficacy of community detection algorithms and the network datasets utilized in our experiments.

(1) Performance Evaluation Metrics: **Accuracy (AC)** [55], or error rate, is the difference between the matrix of community members obtained by an algorithm and that in the real network. It is defined as

$$AC = \|UU^T - U'U'^T\|_F, \tag{15}$$

where U represents the community members obtained by an algorithm and U' denotes the actual community members. The Frobenius norm $\|\cdot\|_F$ is utilized to quantify this difference. The AC is evaluated at each time step; a smaller AC indicates greater accuracy.

Normalized mutual information (NMI) [56] is employed to evaluate the accuracy of a detection model, and is suitable for static networks and those with ground truth values. In this paper, we compute the NMI at each time step. The similarity measure between the community partition obtained from our method and the true community structure is quantified as

$$NMI(U, U') = \frac{\sum_{U,U'} p(U, U') log \frac{U,U'}{p(U)p(U')}}{max(L(U), L(U'))}, \tag{16}$$

where $L(U)$ and $L(U')$ are the respective entropy values of U and U′, which range between 0 and 1. The closer it is to 1, the closer the correlation is to the true result.

F-Score [56] is the harmonic mean of precision and recall. It ranges from 0 to 1, with higher values indicating better precision and recall. The F-Score between detected communities C'_p and real communities C_q can be computed as

$$F(C_q, C'_p) = \frac{2 \times P(C_q, C'_p) \times R(C_q, C'_p)}{P(C_q, C'_p) + R(C_q, C'_p)}. \quad (17)$$

(2) Datasets: We evaluated the performance of TCDA-NE by conducting experiments on selected synthetic and real datasets of representative dynamic complex networks, then compared the results with existing community detection methods.

- **Dataset 1: Dynamic-GN Synthetic Network**
  The GN network, introduced by Girvan et al. [57], is commonly employed for community detection in static networks, which typically consist of 128 or 256 nodes, four communities, and ten time steps. Lin et al. [25] proposed dynamic GN networks incorporating community evolution, where the vertices within each community are randomly reassigned to other communities in predefined proportions. Compared with other networks, the dynamic change of data between time steps is more stable. By changing the parameter settings, it is possible to obtain different dynamic networks for experiments.
- **Dataset 2: Dynamic-LFR Synthetic Network**
  To enhance the resemblance to real-world scenarios, synthetic datasets were generated using a modified version of the Lancichinetti–Fortunato–Radicchi (LFR) model proposed by Greene et al. [58], which uses embedded ground truth communities to generate networks whose internal graphs have similar characteristics in which each graph has community members arranged in a specific way. To thoroughly evaluate the TCDA-NE method, the networks used in our experiments consisted of 1000 nodes over ten time steps, and various parameters were employed to generate distinct network instances. We set the fundamental parameters as follows: μ controlled the mixing parameter that governs the inter-community edge levels, ranging from 0.1 to 0.8; the probability of transitioning between nodes belonging to different communities was fixed at $p = 0.5$; the number of communities was set to 36, with an average node degree of $d = 10$; and the total number of time steps T was set to 10.
- **Dataset 3: KIT-Email Real-World Network**
  The KIT-Email (https://i11www.iti.kit.edu/en/projects/spp1307/emaildata) dataset was constructed based on the contact network derived from email communication within the KIT Information Department. As detailed in Table 1, it comprises 27,887 messages from 1097 email accounts with average degree ranging from 10.10 to 23.72 across temporal snapshots. Each vertex represents an email sender/receiver, with edges denoting message exchanges. Temporal networks were constructed (see topological parameters in Table 1) using 2–6 month intervals, identifying 23–27 communities.
- **Dataset 4: Enron Real-World Network**
  The Enron email corpus (http://www.cs.cmu.edu/~enron/) contains 2001 communications categorized into 12 monthly periods (network statistics in Table 2). With 151 fixed nodes representing user accounts, Table 2 reveals significant monthly variation in edge density (346–1106 edges) and maximum degree (14–59). This dataset's inclusion of erroneous data enables robust evaluation of community detection algorithms under real-world noise conditions.
- **Dataset 5: Cell Real-World Network**
  Derived from the VAST 2008 challenge (http://www.cs.umd.edu/hcil/VASTchallenge08/), this mobile network (parameters in Table 3) contains 400 nodes representing phones with 996–1060 edges across 10 daily time steps. As shown in Table 3, the network maintains stable size (400 nodes) while exhibiting dynamic clustering coefficients (0.0071–0.0239) and maximum degrees (24–35). Call records from June 2006 demonstrate temporal communication patterns through daily network snapshots.

Table 1. Basic parameters of the KIT-Email dataset.

T	Nodes	Edges	Average Degree	Clustering Coefficient	Maximum Degree
1	138	1154	16.72	1.31×10^{14}	39
2	138	1637	23.72	1.31×10^{14}	85
3	138	1554	22.52	0.8293	63
4	138	1210	17.54	6.53×10^{13}	26
5	138	1284	18.61	6.53×10^{13}	28
6	138	1225	17.75	3.26×10^{13}	25
7	138	1289	18.68	3.26×10^{13}	29
8	138	1281	18.57	0.8492	30
9	138	1312	19.01	0.8267	29
10	138	1267	18.36	6.53×10^{13}	26
11	138	1270	18.41	9.79×10^{13}	34
12	138	1315	19.06	3.26×10^{13}	33
13	138	1415	20.51	6.53×10^{13}	35
14	138	1357	19.67	6.53×10^{13}	35
15	138	1281	18.57	3.26×10^{13}	40
16	138	1268	18.38	9.79×10^{13}	36
17	138	1216	17.62	9.79×10^{13}	35
18	138	1271	18.42	3.26×10^{13}	34
19	138	1264	18.32	1.31×10^{14}	34
20	138	1139	16.51	9.79×10^{13}	25
21	138	1011	14.65	9.79×10^{13}	25
22	138	962	13.94	9.79×10^{13}	27
23	138	802	11.62	1.96×10^{14}	20
24	138	697	10.10	3.26×10^{14}	18

Table 2. Basic parameters of the Enron dataset.

T	Nodes	Edges	Average Degree	Clustering Coefficient	Maximum Degree
1	151	346	4.58	2.09×10^{14}	16
2	151	394	5.22	2.39×10^{14}	20
3	151	417	5.52	1.79×10^{14}	16
4	151	497	6.58	2.09×10^{14}	18
5	151	564	4.74	2.68×10^{14}	60
6	151	449	5.95	1.19×10^{14}	14
7	151	492	6.52	1.79×10^{14}	21
8	151	767	10.16	4.47×10^{14}	53
9	151	703	9.31	2.39×10^{14}	38
10	151	1106	14.65	1.79×10^{14}	59
11	151	907	12.01	8.95×10^{13}	34
12	151	631	8.36	2.68×10^{14}	32

Table 3. Basic parameters of the Cell dataset.

T	Nodes	Edges	Average Degree	Clustering Coefficient	Maximum Degree
1	400	1050	5.25	0.0239	33
2	400	998	4.99	0.0139	24
3	400	1018	5.09	0.0101	35
4	400	1028	5.14	0.0136	30
5	400	1016	5.08	0.0119	29
6	400	1024	5.12	0.0149	26
7	400	996	4.98	0.0086	24
8	400	1022	5.11	0.0153	34
9	400	1036	5.18	0.0216	32
10	400	1060	5.30	0.0071	25

4.3. Sensitivity Analysis of Parameters

Parameter sensitivity is critical in machine learning models, as it directly impacts their performance and outcomes. To assess the parameter sensitivity of TCDA-NE, we conducted a series of experiments. For more realistic results, we utilized a dataset from the KIT real-world network. As outlined in Algorithm 1, variation of the parameters α and η in TCDA-NE influences community detection outcomes. We employed the NMI index to quantify the quality of the experimental results.

Figure 2 illustrates the average experimental outcomes of the TCDA-NE model across various time steps considering different parameter configurations. The color and shape in the figure indicate the NMI result of TCDA-NE at the corresponding time as α varies continuously from 0 to 1. As a whole, the NMI value of the experimental results fluctuates within 0.06, indicating that TCDA-NE has weak sensitivity to parameters; thus, the time usually does not require tedious adjustment of the parameters. In addition, the NMI value of the experimental results increases with α and η. When η is greater than 5, the experimental results show little change. In particular, when $\alpha = 0.8$, $\eta = 9$, the model has better community detection results. When α is chosen as 0, the latter term of the model is invalid, which is equivalent to ignoring the case of temporal smoothness. The noticeable decline in the experimental outcomes also signifies the validity of the model.

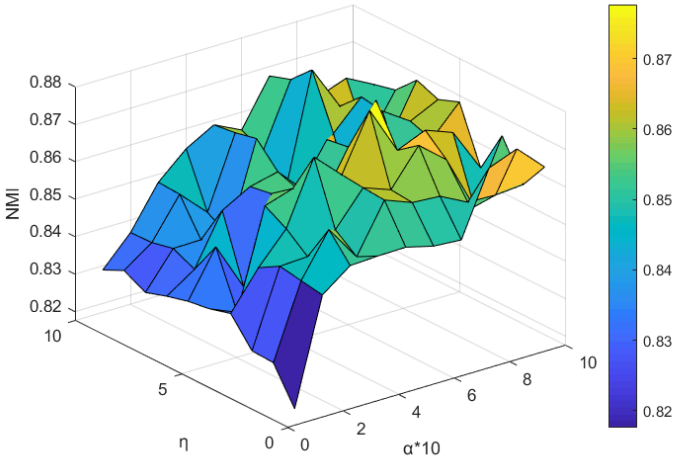


Figure 2. Parameter sensitivity analysis.

4.4. Evaluation of Community Detection Performance

To assess the performance of our model, we conducted a comparative analysis with various baseline models on two categories of synthetic datasets as well as real-world temporal networks.

(1) Analysis of Synthetic Networks: On the Dynamic-GN dataset, we set the average degree to 20 or 21, the transfer rate to [0.1, 0.2, 0.2, 0.1, 0.3], and the network noise to $z = [3, 4, 6, 3, 3]$ over an average of 20 runs. In Figure 3, it can be seen that TCDA-NE, DCNMF, StaNMF, and DECS have the best performance in terms of the NMI metrics, scoring much higher than the other methods, with almost all of them close to 1. However, there are some time steps where the NMI metrics of StaNMF fluctuate, such as the sixth time step in Figure 3a,c and the fourth time step in Figure 3b, while our method suffers little effect because its temporal smoothing correlates adjacent time slices to some extent, eliminating the effect of separate time steps and making the results more robust. At the same time, our method always has a better initialization result than DCNMF.

As can be seen from Figure 4, when the network structure becomes more complex over time, the performance of all methods becomes worse under the condition of high noise. However, for NMI results, TCDA-NE outperforms all other methods in almost all

time steps. Compared with other NMF-based methods, the overall NMI of TCDA-NE is improved by 0.01–0.04.

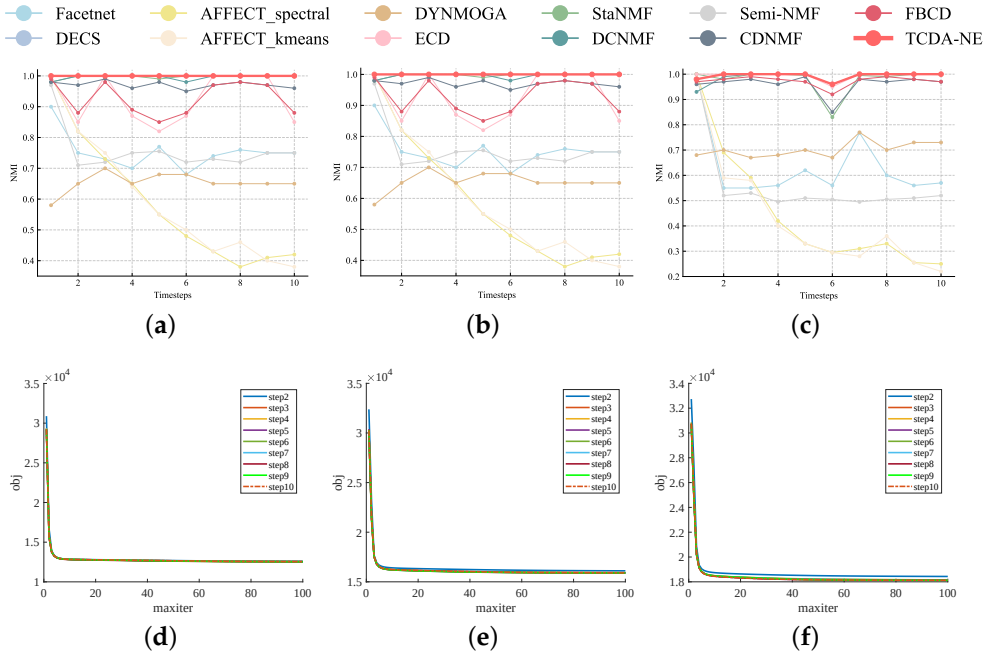


Figure 3. (**a**–**c**) The average NMI result of the Dynamic-GN networks, where the horizontal axis is the time steps: a: z = 3, d = 21, nc = 10%; b: z = 4, c = 21, nc = 20%; c: z = 6, d = 21, nc = 20%. (**d**–**f**) The convergence behavior of the objective function on the corresponding dataset.

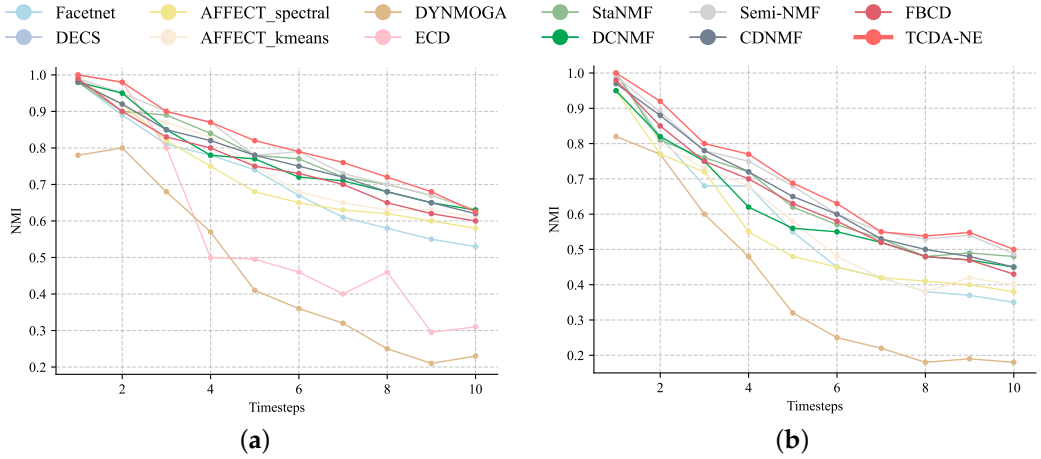


Figure 4. Average NMI result of Dynamic-GN networks: (**a**) z = 3, d = 20, nc = 10%; (**b**) z = 3, c = 20, nc = 30%.

To verify the convergence of the proposed framework, we employed gradient descent and analyzed the results, as shown in Figure 3d–f. Through 100 iterations, we observed that the algorithm consistently converged to a point. This behavior demonstrates that, assuming infinite iterations, the algorithm can ultimately reach the global optimal solution.

Figure 5 shows the results obtained from the temporal network generated using the LFR model, where the network consists of 1000 nodes and exhibits 36 embedded dynamic communities. The values of the parameters were set as $p = 0.5$ and $\mu = 0.7$. Figure 5 shows that TCDA-NE outperforms the other methods. In the left part of Figure 5, the NMI values of the other models reach a maximum of 0.965, while TCDA-NE achieves values ranging from 0.968 to 0.97. In the right part of Figure 5, the performance of TCDA-NE is not outstanding at first, but the results continue to improve with increasing time. In the

fifth to tenth time steps, the NMI results exhibit improvement by 0.01–0.04 compared to the maximum values achieved by other methods. It is noteworthy that the performance consistently excels across all time steps except for the initial one, where the accuracy is lower; this discrepancy can be attributed to the random initialization decomposition of the matrix, with significant improvements observed over time. The proposed model has a low error in most cases, and detects dynamic communities more accurately. These results show that TCDA-NE is more robust than the other methods. The proposed algorithm shows stable convergence, as illustrated in Figure 6.

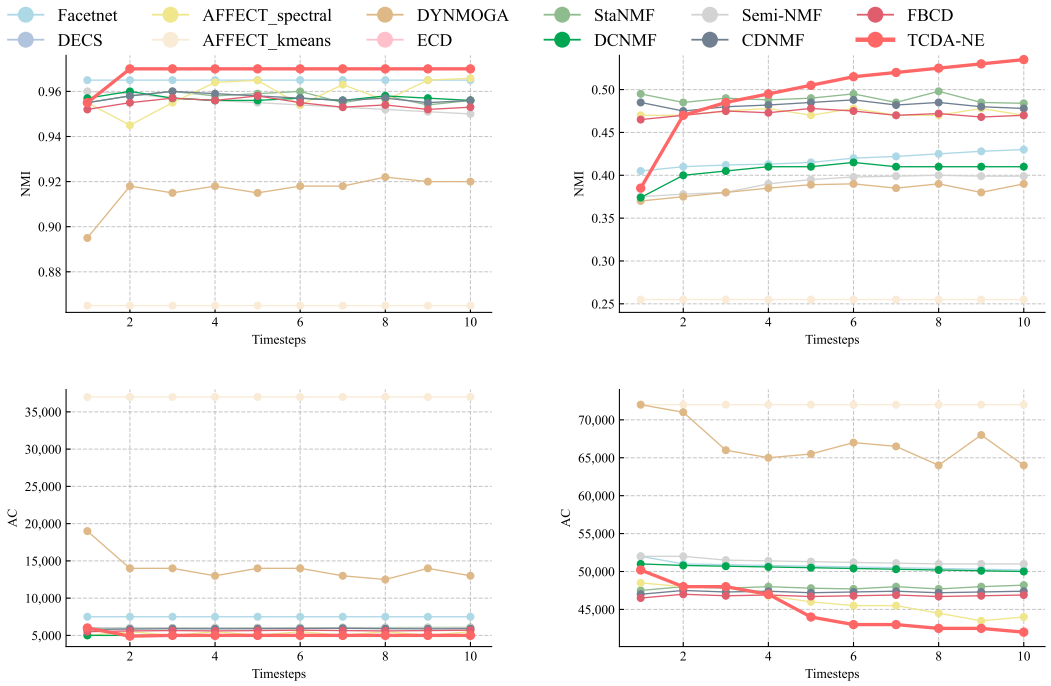


Figure 5. Average NMI and AC results on the Dynamic-LFR dataset. The parameters of the images are as follows: for this image on the left, average degree = 10, mixing parameter $\mu = 0.1$; for the image on the right, average degree = 10, mixing parameter $\mu = 0.7$.

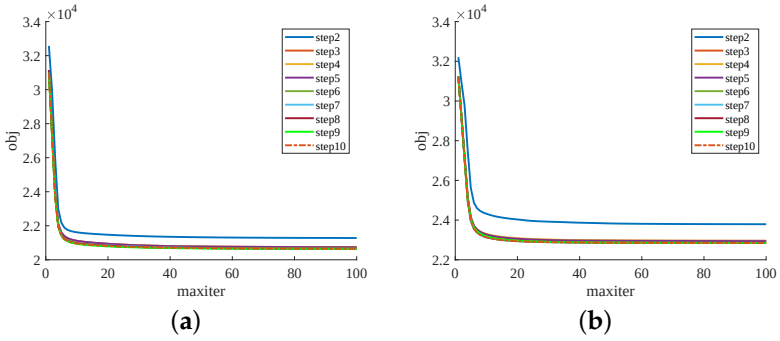


Figure 6. Convergence result of objective function on Dynamic-LFR networks: (**a**) average degree = 10, $\mu = 0.1$; (**b**) average degree = 10, $\mu = 0.7$.

(2) Analysis of Real-World Networks: We utilized the NMI, AC, and F-score to evaluate the performance of different methods on real-world networks. Figure 7 displays the results obtained from the four KIT-Email datasets. We selected KIT datasets with snapshot durations of 2, 3, 4, and 6 months. Based on the results of our analysis of the nodal degree similarity between consecutive time steps, the basic evolutionary clustering framework is more suitable for the KIT dataset. It can be seen that TCDA-NE performs best in most time steps of almost all datasets. For example, considering the NMI, TCDA-NE consistently has

higher scores by a margin of 0.01–0.05. Similar improvements are observed for AC and F-score. TCDA-NE exhibits a notable enhancement compared to DCNMF, highlighting the effectiveness of the multidimensional approximation matrix on real-world networks.

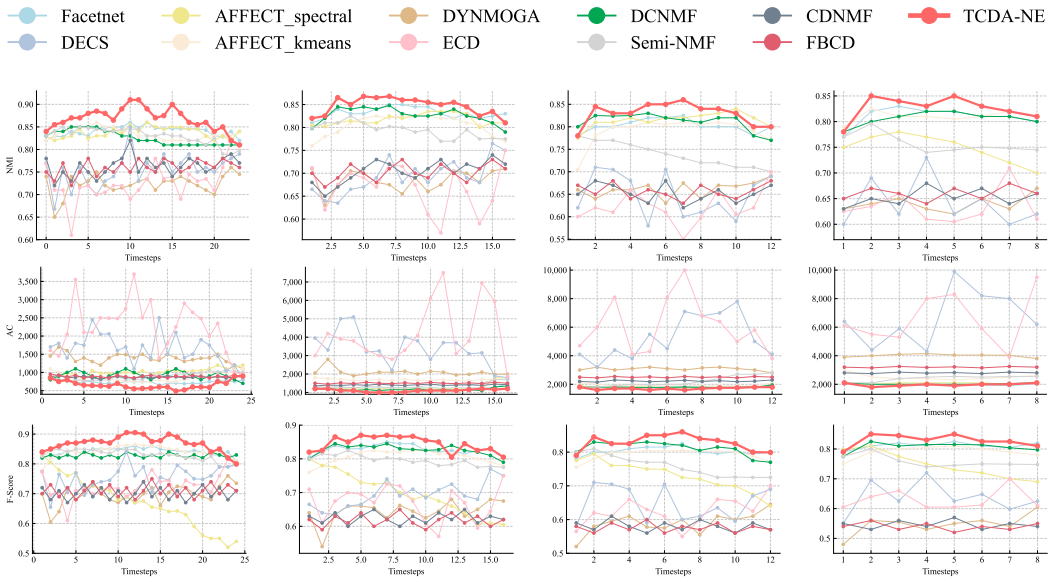


Figure 7. Average results of NMI, AC, and F-score on the KIT-Email dataset. Each column of images represents a separate dataset, with 2, 3, 4, and 6 months as a snapshot from left to right.

The above experiments demonstrated that NMF consistently outperforms the other methods. Therefore, we removed the temporal smoothness constraint for the three NMF methods in order to compare the performance of dynamic and static methods on the Enron and Cell datasets, using line types for dynamic methods and dotted types for static methods. In Figure 8, it can be seen that TCDA-NE outperforms Semi-NMF and DCNMF in terms of both static and dynamic performance. Notably, TCDA-NE consistently performs the best across all datasets, with the difference in NMI values compared to the other two methods ranging from 0.01 to 0.09. This improvement can be attributed to the accuracy of the NE component. Furthermore, the dynamic performance of all methods surpasses their static performance, with an overall increase of approximately 0.01, which can be attributed to time smoothness. We examined the convergence of TCDA-NE on the Cell and Enron datasets, as shown in Figure 9, where the objective function of the algorithm converges.

4.5. Complexity Comparison

TCDA-NE is an iterative method based on the NMF principle; thus, the computational complexity of the model is influenced by that of the network. Networks with more communities, nodes, or edges tend to have longer running times. We conducted a comparative analysis of the computational complexity of the TCDA-NE algorithm. To ensure fairness and reproducible results, all experiments were performed on machines with 8 GB of memory and an Intel Core i5-9300H CPU. Figure 10 shows the runtimes of the different methods on the generated dataset with increasing numbers of nodes. The average degree of all datasets was fixed at 18, and the networks became increasingly sparse as the number of datasets increased. Notably, AFFECT exhibited faster performance on each dataset due to the shrinkage estimation employed in the fusion clustering algorithm. TCDA-NE is better than Facetnet and DYNMOGA with fewer than 512 nodes, after which TCDA-NE has a lower running time than other methods. This is because TCDA-NE must spend extra time on sparse network calculation in order to extract more information in the sparse network; hence, its advantages gradually decrease. An out of time (OOT) error of ECD

and DECS occurs when there are 1024 nodes. Node data above the dotted line indicate that the trial time was too long, but did not affect the observation results. While TCDA-NE is still not fast enough on networks with a large number of nodes, this problem can be solved by neural network or parallel processing technology, which will be the object of our subsequent research.

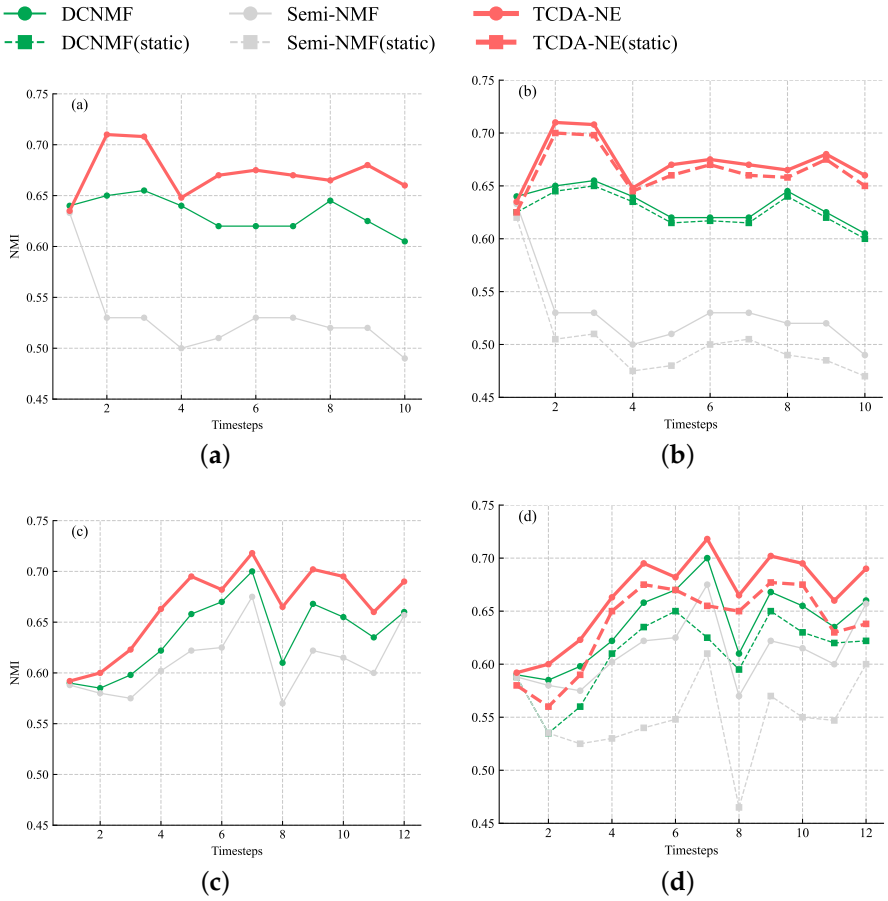


Figure 8. Average NMI result: (**a**,**b**) Cell dataset; (**c**,**d**) Enron dataset.

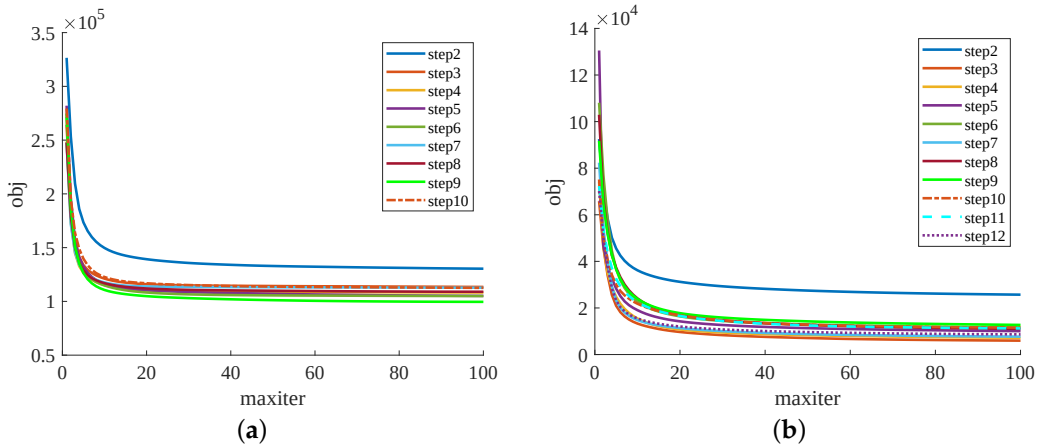


Figure 9. Convergence result of objective function: (**a**) Cell network; (**b**) Enron network.

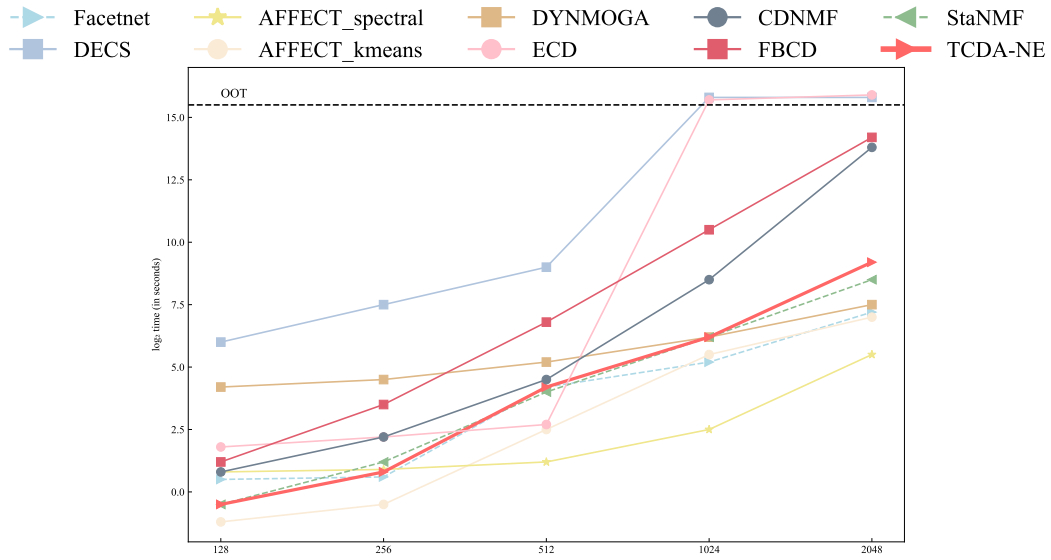


Figure 10. Comparison of running times on composite datasets with different numbers of nodes.

4.6. Ablation Study

Continuing from the previous examination of parameter sensitivity in the TCDA-NE model, it is imperative to delve deeper with an ablation study that provides further insights into the contributions of various components within the model to its overall effectiveness. The results of the ablation study can elucidate the importance of incorporating temporal dynamics and the interplay of different parameters in community detection tasks. In our ablation study, we systematically removed certain components of TCDA-NE to evaluate their individual impacts on the model's performance. By analyzing the outcomes, we aimed to understand which elements are essential for maintaining the integrity and accuracy of community detection. For instance, we performed experiments with and without the temporal smoothness mechanism. The results indicate a significant drop in NMI scores when the temporal smoothness was omitted, reinforcing the notion that the incorporation of time-aware features enhances the model's ability to capture evolving community structures. Moreover, we examined the influence of different embedding techniques utilized within TCDA-NE. By contrasting the outcomes of the model with embedding strategies such as $S^{(1)}$ and $S^{(2)}$, we observed notable variances in community detection results. These findings suggest that the embedding technique can substantially affect the model's performance, emphasizing the need for careful selection based on the specific characteristics of the dataset being analyzed. Additionally, we explored the robustness of TCDA-NE against noisy data. In real-world applications, networks often contain noise that can obscure true community structures. We introduced synthetic noise into our datasets and reassessed the performance of TCDA-NE. The model demonstrated a commendable level of resilience, maintaining relatively stable NMI scores even under adverse conditions. This robustness is a crucial attribute for any community detection model intended for real-world applications where data quality cannot always be guaranteed.

Table 4 provides valuable insights into the critical components of the TCDA-NE model and their impacts on performance across different datasets. The full TCDA-NE model achieved the highest NMI and F-score metrics across all three datasets, indicating the strong performance of the TCDA-NE model on community detection tasks. When removing the interaction terms, the NMI and F-score decreased by 0.02, 0.03, and 0.04 on the three datasets, respectively. This suggests that the interaction terms are an important component of the TCDA-NE model, contributing to its improved detection capability. When removing the temporal smoothness mechanism, the NMI and F-score saw more significant drops

of 0.04, 0.07, and 0.08 on the three datasets. This highlights the importance of temporal features in dynamic community detection and underscores the advantage of TCDA-NE in leveraging temporal information. Overall, removing either of the interaction terms or the temporal smoothness mechanism resulted in performance degradation for the TCDA-NE model, indicating that these two components play crucial roles and are key factors contributing to the excellent performance of TCDA-NE.

Table 4. Ablation study results (NMI scores).

Dataset		KIT	Cell	Enron
Full TCDA-NE	NMI	0.87	0.71	0.78
	F-score	0.86	0.70	0.76
w/o Interaction Terms	NMI	0.85	0.68	0.74
	F-score	0.84	0.67	0.73
w/o Temporal Smoothness	NMI	0.83	0.64	0.70
	F-score	0.83	0.65	0.70

5. Discussion and Conclusions

Temporal community detection and analysis have garnered significant attention in the field of complex networks due to their continuous evolution and advancement. Detecting community structures in dynamic networks plays a crucial role in predicting and analyzing future changes in their structure and functionality. In this paper, we have introduced the TCDA-NE method for temporal community detection, which uses evolutionary clustering to integrate the community structure of dynamic networks into network embedding. This approach effectively addresses data sparsity in complex networks and enables the learned nodes to preserve both the microstructure and community structure.

In our experiments, we compared the efficacy of TCDA-NE with several other dynamic community detection algorithms. TCDA-NE outperformed the other methods on both synthetic and real-world networks, demonstrating superior accuracy in community detection within temporal networks. By eliminating time smoothness constraints and leveraging the combination of NMF and evolutionary clustering, TCDA-NE exhibits a clear advantage over other NMF methods in terms of both static and dynamic performance.

The implications of these findings extend beyond mere performance metrics, offering significant avenues for future research. One potential direction is the exploration of hybrid models that leverage the strengths of TCDA-NE in combination with other state-of-the-art community detection algorithms. For example, integrating the temporal dimension of TCDA-NE with density-based approaches could provide a more holistic understanding of community evolution in dynamic networks. Additionally, we propose the development of adaptive algorithms capable of automatically tuning parameters such as α and η based on real-time data characteristics. Such advancements could minimize the need for manual tuning, thereby enhancing the applicability of TCDA-NE across diverse scenarios ranging from social network analysis to biological networks.

Furthermore, expanding TCDA-NE to accommodate large-scale networks and exploring its potential applications beyond social networks, for example in biological and financial systems, presents promising directions for future work. By continuously refining the model to adapt to the complexities of real-world data, we can significantly enhance the efficacy of community detection tasks, thereby contributing to the broader fields of machine learning and network analysis. As this research area progresses, it will be crucial

to remain open to emerging methodologies that can complement our findings and push the boundaries of what is achievable in community detection for dynamic networks.

Author Contributions: Conceptualization, L.Y. and Y.K.; Methodology, L.Y., X.Z. and Y.K.; Software, X.Z. and Z.L.; Validation, L.Y.; Investigation, X.Z. and Y.K.; Resources, L.Y.; Writing—original draft, L.Y.; Writing—review & editing, L.Y., X.Z., Y.K., Z.L. and X.L.; Supervision, X.L. and C.L.; Project administration, X.L. and C.L. All authors have read and agreed to the published version of the manuscript.

Funding: This work was supported by Bingtuan Science and Technology Programs (2024AB080, 2023CB005, 2023ZD066, 2022CB002-08). The research was conducted at the National Security Research Institute, Shihezi University, China.

Data Availability Statement: The original contributions presented in this study are included in the article. Further inquiries can be directed to the corresponding authors.

Conflicts of Interest: The authors declare no conflicts of interest.

References

1. Zhu, J.; Wei, D. Analysis of stock market based on visibility graph and structure entropy. *Phys. Stat. Mech. Appl.* **2021**, *576*, 126036. [CrossRef]
2. Zhang, H.; Wang, C.D.; Lai, J.H.; Yu, P.S. Modularity in complex multilayer networks with multiple aspects: A static perspective. In *Applied Informatics*; SpringerOpen: Berlin/Heidelberg, Germay, 2017; Volume 4, pp. 1–29.
3. Tran, D.T.; Iosifidis, A.; Kanniainen, J.; Gabbouj, M. Temporal attention-augmented bilinear network for financial time-series data analysis. *IEEE Trans. Neural Netw. Learn. Syst.* **2018**, *30*, 1407–1418. [CrossRef]
4. Ye, F.; Chen, C.; Zheng, Z. Deep autoencoder-like nonnegative matrix factorization for community detection. In Proceedings of the 27th ACM International Conference on Information and Knowledge Management, Lingotto, Italy, 22–26 October 2018; pp. 1393–1402.
5. Mucha, P.J.; Richardson, T.; Macon, K.; Porter, M.A.; Onnela, J.P. Community structure in time-dependent, multiscale, and multiplex networks. *Science* **2010**, *328*, 876–878. [CrossRef]
6. Yang, T.; Chi, Y.; Zhu, S.; Gong, Y.; Jin, R. Detecting communities and their evolutions in dynamic social networks—A Bayesian approach. *Mach. Learn.* **2011**, *82*, 157–189. [CrossRef]
7. Qiu, J.; Dong, Y.; Ma, H.; Li, J.; Wang, C.; Wang, K.; Tang, J. Netsmf: Large-scale network embedding as sparse matrix factorization. In *The World Wide Web Conference*; Association for Computing Machinery: New York, NY, USA, 2019; pp. 1509–1520.
8. Wu, Z.; Pan, S.; Chen, F.; Long, G.; Zhang, C.; Philip, S.Y. A comprehensive survey on graph neural networks. *IEEE Trans. Neural Netw. Learn. Syst.* **2020**, *32*, 4–24. [CrossRef] [PubMed]
9. Zhang, D.; Yin, J.; Zhu, X.; Zhang, C. Network representation learning: A survey. *IEEE Trans. Big Data* **2018**, *6*, 3–28. [CrossRef]
10. Zhang, Z.; Cui, P.; Zhu, W. Deep learning on graphs: A survey. *IEEE Trans. Knowl. Data Eng.* **2020**, *34*, 249–270. [CrossRef]
11. Guo, J.; Xu, L.; Liu, J. SPINE: structural identity preserved inductive network embedding. *arXiv* **2018**, arXiv:1802.03984
12. Liu, X.X.; Wang, K.; Wang, C.D.; Huang, L. Attention-based Multi-proximity Preserved Attributed Network Embedding. In Proceedings of the 2021 International Joint Conference on Neural Networks (IJCNN), Virtual, 18–22 July 2021; pp. 1–8.
13. Zhu, Z.; Li, X.; Liu, K.; Li, Q. Dropping symmetry for fast symmetric nonnegative matrix factorization. *Adv. Neural Inf. Process. Syst.* **2018**, *31*, 1–11.
14. Liang, N.; Yang, Z.; Li, Z.; Sun, W.; Xie, S. Multi-view clustering by non-negative matrix factorization with co-orthogonal constraints. *Knowl.-Based Syst.* **2020**, *194*, 105582. [CrossRef]
15. Ortega-Martorell, S.; Lisboa, P.J.; Vellido, A.; Simões, R.V.; Pumarola, M.; Julià-Sapé, M.; Arús, C. Convex non-negative matrix factorization for brain tumor delimitation from MRSI data. *PLoS ONE* **2012**, *7*, e47824. [CrossRef]
16. Li, G.; Zhang, X.; Zheng, S.; Li, D. Semi-supervised convex nonnegative matrix factorizations with graph regularized for image representation. *Neurocomputing* **2017**, *237*, 1–11. [CrossRef]
17. Yang, Q.; Wei, W.; Zhang, R.; Pang, B.; Feng, X. Enhance Ambiguous Community Structure via Multi-strategy Community Related Link Prediction Method with Evolutionary Process. *arXiv* **2022**, arXiv:2204.13301.
18. Cha, J.; Kim, S.; Park, E. A lexicon-based approach to examine depression detection in social media: The case of Twitter and university community. *Humanit. Soc. Sci. Commun.* **2022**, *9*, 1–10. [CrossRef]
19. Odhiambo, L.A.; Anaba, E.; Stephens, P.C.; Cheruvu, V.K.; Zullo, M.D. Community-Based Approach to Assess Obstructive Respiratory Diseases and Risk in Urban African American Churches. *J. Immigr. Minor. Health* **2023**, *25*, 389–397. [CrossRef] [PubMed]

20. Bala, V.; Duesterwald, E.; Banerjia, S. Dynamo: A transparent dynamic optimization system. In Proceedings of the ACM SIGPLAN 2000 Conference on Programming Language Design and Implementation, Vancouver, BC, Canada, 18–21 June 2000; pp. 1–12.
21. Traag, V.A.; Waltman, L.; Van Eck, N.J. From Louvain to Leiden: Guaranteeing well-connected communities. *Sci. Rep.* **2019**, *9*, 5233. [CrossRef] [PubMed]
22. McGann, D.; Rogers, J.G., III; Kaess, M. Robust Incremental Smoothing and Mapping (riSAM). *arXiv* **2022**, arXiv:2209.14359.
23. Saini, R.; Mussbacher, G.; Guo, J.L.; Kienzle, J. Machine learning-based incremental learning in interactive domain modelling. In Proceedings of the 25th International Conference on Model Driven Engineering Languages and Systems, Montreal, QC, Canada, 16–21 October 2022; pp. 176–186.
24. Li, J.; Wu, Q.; Li, L.; Sun, R.; Mu, H.; Zhao, K. Incremental clustering algorithm based on representative points and covariance for large data. *Int. J. Simul. Process. Model.* **2023**, *20*, 113–124. [CrossRef]
25. Ma, X.; Dong, D. Evolutionary nonnegative matrix factorization algorithms for community detection in dynamic networks. *IEEE Trans. Knowl. Data Eng.* **2017**, *29*, 1045–1058. [CrossRef]
26. Liu, F.; Wu, J.; Xue, S.; Zhou, C.; Yang, J.; Sheng, Q. Detecting the evolving community structure in dynamic social networks. *World Wide Web* **2020**, *23*, 715–733. [CrossRef]
27. Yin, Y.; Zhao, Y.; Li, H.; Dong, X. Multi-objective evolutionary clustering for large-scale dynamic community detection. *Inf. Sci.* **2021**, *549*, 269–287. [CrossRef]
28. Martinet, L.E.; Kramer, M.; Viles, W.; Perkins, L.; Spencer, E.; Chu, C.; Cash, S.; Kolaczyk, E. Robust dynamic community detection with applications to human brain functional networks. *Nat. Commun.* **2020**, *11*, 1–13. [CrossRef]
29. Şapcı, A.O.; Lu, S.; Tastan, O.; Keleş, S. MuDCoD: Multi-Subject Community Detection in Personalized Dynamic Gene Networks from Single Cell RNA Sequencing. *bioRxiv* **2021**, *39*, btad592. [CrossRef]
30. Choong, J.J.; Liu, X.; Murata, T. Variational approach for learning community structures. *Complexity* **2018**, *2018*, 4867304. [CrossRef]
31. Sewell, D.K.; Chen, Y. Latent space approaches to community detection in dynamic networks. *Bayesian Anal.* **2017**, *12*, 351–377. [CrossRef]
32. Passino, F.S.; Heard, N.A. Bayesian estimation of the latent dimension and communities in stochastic blockmodels. *Stat. Comput.* **2020**, *30*, 1291–1307. [CrossRef]
33. Akcay, S.; Atapour-Abarghouei, A.; Breckon, T.P. Ganomaly: Semi-supervised anomaly detection via adversarial training. In Proceedings of the Asian Conference on Computer Vision, Perth, Australia, 2–6 December 2018; Springer: Berlin/Heidelberg, Germany, 2018, pp. 622–637.
34. Rusanen, J.; Hietanen, M.; Sethi, A.; Rahkonen, T.; Pärssinen, A.; Aikio, J.P. Ka-Band stacked power amplifier on 22 nm CMOS FDSOI technology utilizing back-gate bias for linearity improvement. In Proceedings of the 2019 IEEE Nordic Circuits and Systems Conference (NORCAS): NORCHIP and International Symposium of System-on-Chip (SoC), Helsinki, Finland, 29–30 October 2019; pp. 1–4.
35. Gu, X.; Chen, X.; Yang, M.; Du, Y.; Tang, M. Bi-DNE: Bilayer evolutionary pattern preserved embedding for dynamic networks. *Complex Intell. Syst.* **2024**, *10*, 3763–3788. [CrossRef]
36. Schaub, M.T.; Segarra, S.; Tsitsiklis, J.N. Blind identification of stochastic block models from dynamical observations. *SIAM J. Math. Data Sci.* **2020**, *2*, 335–367. [CrossRef]
37. Junuthula, R.; Haghdan, M.; Xu, K.S.; Devabhaktuni, V. The block point process model for continuous-time event-based dynamic networks. In Proceedings of the The World Wide Web Conference, San Francisco, CA, USA, 13–17 May 2019; pp. 829–839.
38. Jing, B.Y.; Li, T.; Lyu, Z.; Xia, D. Community detection on mixture multilayer networks via regularized tensor decomposition. *Ann. Stat.* **2021**, *49*, 3181–3205. [CrossRef]
39. Cao, S.; Lu, W.; Xu, Q. Grarep: Learning graph representations with global structural information. In Proceedings of the 24th ACM International on Conference on Information and Knowledge Management, Melbourne, Australia, 19–23 October 2015; pp. 891–900.
40. Yang, Y.; Ning, N.; Zhang, Y.; Wu, B. Community preserving node embedding based on seed-expansion sampling. In Proceedings of the 2019 IEEE Fourth International Conference on Data Science in Cyberspace (DSC), Hangzhou, China, 23–25 June 2019; pp. 459–465.
41. Duan, Z.; Sun, X.; Zhao, S.; Chen, J.; Zhang, Y.; Tang, J. Hierarchical community structure preserving approach for network embedding. *Inf. Sci.* **2021**, *546*, 1084–1096. [CrossRef]
42. Jiao, P.; Li, T.; Wu, H.; Wang, C.D.; He, D.; Wang, W. HB-DSBM: Modeling the Dynamic Complex Networks From Community Level to Node Level. *IEEE Trans. Neural Netw. Learn. Syst.* **2022**, *34*, 8310–8323. [CrossRef] [PubMed]
43. Tian, Q.; Pan, L.; Zhang, W.; Li, T.; Wu, H.; Jiao, P.; Wang, W. Lower order information preserved network embedding based on non-negative matrix decomposition. *Inf. Sci.* **2021**, *572*, 43–56. [CrossRef]

44. Kwak, G.H.; Park, C.w.; Lee, K.d.; Na, S.i.; Ahn, H.y.; Park, N.W. Potential of hybrid CNN-RF model for early crop mapping with limited input data. *Remote Sens.* **2021**, *13*, 1629. [CrossRef]
45. Wu, Y.; Jiang, M.; Lei, J.; Xu, H. Named entity recognition in Chinese clinical text using deep neural network. *Stud. Health Technol. Informatics* **2015**, *216*, 624.
46. Shen, X.; Dai, Q.; Mao, S.; Chung, F.l.; Choi, K.S. Network together: Node classification via cross-network deep network embedding. *IEEE Trans. Neural Netw. Learn. Syst.* **2020**, *32*, 1935–1948. [CrossRef] [PubMed]
47. Kan, S.; Cen, Y.; Li, Y.; Vladimir, M.; He, Z. Local Semantic Correlation Modeling Over Graph Neural Networks for Deep Feature Embedding and Image Retrieval. *IEEE Trans. Image Process.* **2022**, *31*, 2988–3003. [CrossRef]
48. Kojaku, S.; Radicchi, F.; Ahn, Y.Y.; Fortunato, S. Network community detection via neural embeddings. *Nat. Commun.* **2024**, *15*, 9446. [CrossRef] [PubMed]
49. Blackman, L.; Venn, C. Affect. *Body Soc.* **2010**, *16*, 7–28. [CrossRef]
50. Xu, X.; Gu, R.; Dai, F.; Qi, L.; Wan, S. Multi-objective computation offloading for internet of vehicles in cloud-edge computing. *Wirel. Netw.* **2020**, *26*, 1611–1629. [CrossRef]
51. Li, Y.; Chen, J.; Chen, C.; Yang, L.; Zheng, Z. Contrastive deep nonnegative matrix factorization for community detection. In Proceedings of the ICASSP 2024-2024 IEEE International Conference on Acoustics, Speech and Signal Processing (ICASSP), Seoul, Korea, 14–19 April 2024; pp. 6725–6729.
52. Gmati, H.; Mouakher, A.; Gonzalez-Pardo, A.; Camacho, D. A new algorithm for communities detection in social networks with node attributes. *J. Ambient. Intell. Humaniz. Comput.* **2024**, *15*, 1779–1791. [CrossRef]
53. Wu, S.; Joseph, A.; Hammonds, A.S.; Celniker, S.E.; Yu, B.; Frise, E. Stability-driven nonnegative matrix factorization to interpret spatial gene expression and build local gene networks. *Proc. Natl. Acad. Sci. USA* **2016**, *113*, 4290–4295. [CrossRef]
54. Peng, S.; Yang, Z.; Ling, B.W.K.; Chen, B.; Lin, Z. Dual semi-supervised convex nonnegative matrix factorization for data representation. *Inf. Sci.* **2022**, *585*, 571–593. [CrossRef]
55. Lin, Y.R.; Chi, Y.; Zhu, S.; Sundaram, H.; Tseng, B.L. Analyzing communities and their evolutions in dynamic social networks. *ACM Trans. Knowl. Discov. Data (TKDD)* **2009**, *3*, 1–31. [CrossRef]
56. Jing, L.; Ng, M.K.; Huang, J.Z. An entropy weighting k-means algorithm for subspace clustering of high-dimensional sparse data. *IEEE Trans. Knowl. Data Eng.* **2007**, *19*, 1026–1041. [CrossRef]
57. Girvan, M.; Newman, M.E. Community structure in social and biological networks. *Proc. Natl. Acad. Sci. USA* **2002**, *99*, 7821–7826. [CrossRef] [PubMed]
58. Greene, D.; Doyle, D.; Cunningham, P. Tracking the evolution of communities in dynamic social networks. In Proceedings of the 2010 International Conference on Advances in Social Networks Analysis and Mining, Odense, Denmark, 9–11 August 2010; pp. 176–183.

Disclaimer/Publisher's Note: The statements, opinions and data contained in all publications are solely those of the individual author(s) and contributor(s) and not of MDPI and/or the editor(s). MDPI and/or the editor(s) disclaim responsibility for any injury to people or property resulting from any ideas, methods, instructions or products referred to in the content.